

Carbon-Smart Synthesis of Bioactive Chalcones With Molecular Docking-Guided Antimicrobial Lead Identification

Haresh ram^a, Kaushik joshi^b, Ami ravaliya^b, Bhavesh Dodiya^c, Govind kher^a and Ritesh tandel^a

^aDepartment of chemistry, Tolani College of arts & science, Adipur, Kutch, Gujarat, India

^bDepartment of chemistry, Doshi Kalidas Virji Arts & Science College, Jamnagar, Gujarat, India

^cDepartment of chemistry, Government Science College, Mandvi, Kutch, Gujarat, India

*Corresponding Author: kajoshi@sauuni.ac.in

Received: 28th Feb, 2026; Revised: 6th March 2026; Accepted: 7th April, 2026; Available Online: 20th April, 2026

ABSTRACT

A new series of chalcone derivatives containing a benzothiophene moiety were synthesized via a base-catalyzed Claisen–Schmidt condensation reaction. The synthetic strategy involved the condensation of 2-methyl-1-benzothiophene-3-carbaldehyde with various substituted acetophenones in the presence of sodium hydroxide using methanol as a solvent. The reaction proceeded smoothly to afford the corresponding (E)-1-(substituted phenyl)-3-(2-methylbenzothiophen-3-yl)prop-2-en-1-one derivatives in good to excellent yields. Different electron-withdrawing and electron-donating substituents such as Cl, F, OCH₃, CH₃, and H on the aromatic ring were explored to study their influence on the reaction outcome. The structures of the synthesized compounds were confirmed by spectral techniques including FT-IR, ¹H NMR, ¹³C NMR, and mass spectrometry. The presence of the α,β -unsaturated carbonyl system along with the benzothiophene nucleus makes these compounds promising scaffolds for further biological evaluation.

Keywords: Chalcone derivatives, Benzothiophene, Claisen-Schmidt condensation, Antimicrobial activity.

How to cite this article: (Rama H, Joshi K, Ravaliya A, Dodiya B, Khera G, Tandela R), (Carbon-Smart Synthesis of Bioactive Chalcones with Molecular Docking-Guided Antimicrobial Lead Identification). Int J Drug Deliv Technol. 2026;16(5): 233-244. DOI: 10.25258/ijddt.16.5.26

Source of support: Nil.

Conflict of interest: None

INTRODUCTION

Chalcones are an important class of α,β -unsaturated carbonyl compounds characterized by the general framework 1,3-diaryl-2-propen-1-one (Ar–CO–CH=CH–Ar). Due to the presence of a highly conjugated enone system, chalcones exhibit remarkable chemical reactivity and serve as valuable intermediates for the synthesis of numerous heterocyclic scaffolds. In recent years, chalcone derivatives have gained significant attention in medicinal chemistry because of their broad spectrum of pharmacological activities and their ability to act as privileged scaffolds for structural modification and optimization.

A comprehensive review by Elkanzi et al. (2022) in the synthesis of chalcone derivatives containing N, O and/or S heterocycles, and summarized their diverse biological applications including anticancer, antimicrobial, anti-inflammatory, antioxidant, and antidiabetic activities, confirming the chalcone nucleus as a versatile pharmacophore for drug discovery.[1] Furthermore, green and sustainable synthetic approaches for chalcone preparation have also been emphasized recently. Marotta et al. (2022) reviewed eco-friendly methodologies such as solvent-free reactions, mechanochemical protocols, and other green routes, indicating that chalcones are not only

biologically important but also compatible with modern sustainable chemistry principles. [5]

Recent experimental studies further validate the biomedical relevance of chalcone-based hybrids. For example, Baramaki et al. (2024) reported a new series of indole-chalcone hybrids exhibiting significant analgesic and anti-inflammatory activity in vivo, strengthening the role of chalcone conjugates in inflammation-related therapy.[2] Similarly, Aboukhatwa et al. (2023) designed chalcone–sulfonamide hybrids which demonstrated notable anticancer activity, providing an example of chalcone-based multitargeted strategies.[3] In another important contribution, Leechaisit et al. (2023) developed novel naphthoquinone–chalcone hybrids showing promising cytotoxic activity against various cancer cell lines, highlighting chalcones as effective scaffolds in oncology-oriented drug development.[4] Additionally, chalcone derivatives and their metal complexes have also been reported as biologically significant compounds; Kaushal et al. (2021) reviewed their biomedical potential, especially for antidiabetic applications involving enzyme inhibition mechanisms.[7] Modern medicinal chemistry emphasizes hybrid molecule strategies, such as thiazole–sulfonamide hybrid structures that demonstrate promising anticancer activity through dual inhibition mechanisms,

*Author for Correspondence: kajoshi@sauuni.ac.in

highlighting the importance of multifunctional scaffolds in drug discovery [6].

Chalcones (α,β -unsaturated ketones) are an important class of natural and synthetic compounds known for their broad pharmacological potential. In recent years, chalcone derivatives have gained significant attention as promising bioactive scaffolds, particularly due to their strong antifungal activity. Gupta and Jain reported the synthesis and evaluation of chalcone derivatives as potential antifungal agents, confirming their medicinal importance [8]. Further, novel vanillin-based chalcones were developed and investigated for antifungal activity supported by DFT calculations, helping to understand structure–activity relationships [9]. The chalcone framework is highly versatile and serves as a key precursor for synthesizing various heterocyclic systems such as pyrazoles, which often enhance biological activity. A comprehensive review highlighted that chalcones exhibit diverse biological properties including antimicrobial, anti-inflammatory, antioxidant, and anticancer activities [10]. With the integration of computational tools, a Curcumin Chalcone Derivatives Database (CCDD) was introduced, offering a valuable platform for systematic analysis of natural chalcone derivatives [11]. Moreover, newly designed chalcone derivatives containing specific functional moieties have shown improved activities, such as anticancer and antioxidant properties [12]. Recent studies have also focused on chalcones in relation to drug resistance mechanisms; for example, acridine-based chalcones and their interactions with ABC transporters have been explored, indicating their potential relevance in overcoming multidrug resistance and advancing drug discovery [13].

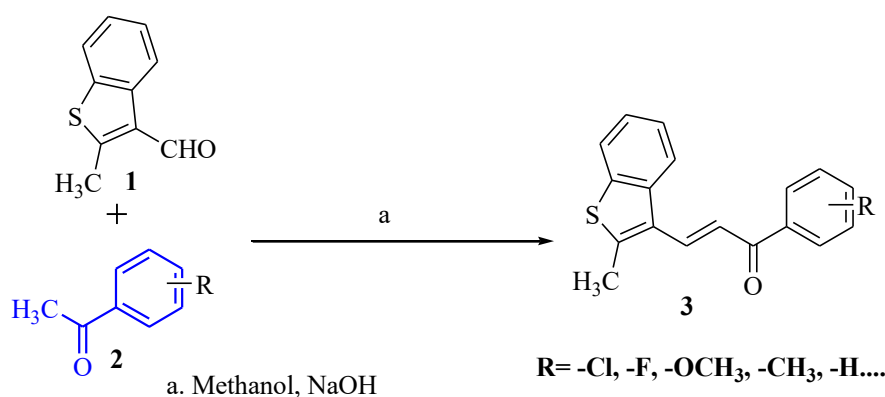


fig. 1 the scheme of Benzothiophene-Based Chalcone Derivatives

The synthetic pathway for the preparation of the target compounds is illustrated in Scheme 1. The reaction involves a base-catalyzed Claisen–Schmidt condensation between 2-methyl-1-benzothiophene-3-carbaldehyde and various substituted acetophenones in methanol. The reaction proceeds via enolate ion formation followed by nucleophilic addition and subsequent dehydration to yield the corresponding (E)- α,β -unsaturated ketones. Different substituents (Cl, F, OCH₃, CH₃, and H) on the phenyl ring

MATERIALS AND METHODS

All chemicals and reagents were of analytical grade and used without further purification. 2-Methyl-1-benzothiophene-3-carbaldehyde and substituted acetophenones were procured from commercial suppliers. Methanol was used as the reaction solvent, and sodium hydroxide pellets were employed as the base catalyst. Reaction progress was monitored by thin-layer chromatography (TLC) using silica gel plates with ethyl acetate–hexane as the eluent. Melting points were determined in open capillary tubes and are uncorrected.

FT-IR spectra were recorded using KBr pellets. ¹H NMR and ¹³C NMR spectra were recorded in DMSO-d₆ using TMS as an internal standard. Mass spectra were obtained using ESI-MS.

EXPERIMENTAL SECTION

General Procedure for the Synthesis of Benzothiophene-Based Chalcone Derivatives (3a-j)

To a stirred solution of 2-methyl-1-benzothiophene-3-carbaldehyde (1 mmol) in methanol (20 mL), an equimolar amount (1 mmol) of substituted acetophenone was added. To this mixture, aqueous sodium hydroxide solution (10%, 3–4 mL) was added dropwise with continuous stirring at room temperature.

The reaction mixture was stirred for 4–6 h and monitored by TLC. Upon completion of the reaction, the mixture was poured into crushed ice and neutralized with dilute hydrochloric acid. The resulting solid precipitate was filtered, washed with cold water, dried, and recrystallized from methanol to afford the pure chalcone derivatives (3a–j).

were introduced to generate structural diversity within the synthesized series.

(E)-1-(4-chlorophenyl)-3-(2-methylbenzo[b]thiophen-3-yl)prop-2-en-1-one (3a)

The ¹H NMR spectrum of the synthesized chalcone derivative is consistent with the proposed structure, showing aromatic proton multiplets in the range δ 7.08–8.19 ppm and two trans-coupled olefinic doublets at δ 7.40–7.80 ppm ($J \approx 15$ –16 Hz), confirming the α,β -

unsaturated carbonyl system. A singlet at δ 2.19–2.49 ppm corresponds to the methyl group on the benzothiophene ring. The IR spectrum further supports the structure with a strong C=O stretching band at 1673 cm^{-1} along with characteristic aromatic C–H and C=C vibrations. The mass spectrum exhibits a molecular ion peak at m/z 312, corresponding to the molecular weight of the compound. Elemental analysis is in good agreement with the proposed molecular formula $\text{C}_{18}\text{H}_{13}\text{ClOS}$ (MW = 312.81): calcd C, 69.10; H, 4.19; Cl, 11.33; O, 5.11; S, 10.25%; found C, 69.13; H, 4.17; Cl, 11.34; O, 5.10; S, 10.22%.

(E)-1-(3-chlorophenyl)-3-(2-methylbenzo[b]thiophen-3-yl)prop-2-en-1-one (3b)

The ^1H NMR spectrum of the synthesized chalcone derivative is consistent with the proposed structure, showing aromatic proton multiplets in the range δ 7.03–8.03 ppm and two trans-coupled olefinic doublets at δ 7.43–7.89 ppm ($J \approx 15$ –16 Hz), confirming the α,β -unsaturated carbonyl system. A singlet at δ 2.12–2.46 ppm corresponds to the methyl group on the benzothiophene ring. The IR spectrum further supports the structure with a strong C=O stretching band at 1671 cm^{-1} along with characteristic aromatic C–H and C=C vibrations. The mass spectrum exhibits a molecular ion peak at m/z 312, corresponding to the molecular weight of the compound. Elemental analysis is in good agreement with the proposed molecular formula $\text{C}_{18}\text{H}_{13}\text{ClOS}$ (MW = 312.81): calcd C, 69.10; H, 4.19; Cl, 11.33; O, 5.11; S, 10.25%; found C, 69.11; H, 4.12; Cl, 11.31; O, 5.12; S, 10.28%.

(E)-1-(2-chlorophenyl)-3-(2-methylbenzo[b]thiophen-3-yl)prop-2-en-1-one (3c)

The ^1H NMR spectrum of the synthesized chalcone derivative is consistent with the proposed structure, exhibiting aromatic proton multiplets in the region δ 7.10–8.25 ppm and two trans-coupled olefinic doublets at δ 7.45–7.85 ppm ($J \approx 15$ –16 Hz), confirming the α,β -unsaturated carbonyl system. A singlet at δ 2.22–2.50 ppm corresponds to the methyl group on the benzothiophene ring. The IR spectrum shows a characteristic strong C=O stretching band at ~ 1672 cm^{-1} along with aromatic C–H and C=C stretching vibrations. The mass spectrum displays a molecular ion peak at m/z 312, consistent with the molecular weight of the compound. Elemental analysis supports the proposed molecular formula $\text{C}_{18}\text{H}_{13}\text{ClOS}$ (MW = 312.81): calcd C, 69.10; H, 4.19; Cl, 11.33; O, 5.11; S, 10.25%; found C, 69.05; H, 4.10; Cl, 11.38; O, 5.15; S, 10.20%.

(E)-1-(4-fluorophenyl)-3-(2-methylbenzo[b]thiophen-3-yl)prop-2-en-1-one (3d)

The ^1H NMR spectrum of the synthesized chalcone derivative is consistent with the proposed structure. It exhibits aromatic proton multiplets in the region δ 7.05–8.20 ppm corresponding to the phenyl and benzothiophene aromatic protons. Two characteristic trans-coupled olefinic doublets appear at δ 7.40–7.80 ppm ($J \approx 15$ –16 Hz) confirming the presence of the α,β -unsaturated carbonyl (chalcone) system. A singlet at δ 2.20–2.45 ppm corresponds to the methyl group

attached to the benzothiophene ring. The IR spectrum shows a strong C=O stretching band around ~ 1668 cm^{-1} , characteristic of the conjugated chalcone carbonyl group, along with aromatic C–H stretching (~ 3030 cm^{-1}) and C=C stretching bands (~ 1580 – 1600 cm^{-1}). The mass spectrum shows a molecular ion peak at m/z 296, consistent with the molecular weight of the compound. Elemental analysis supports the proposed molecular formula $\text{C}_{18}\text{H}_{13}\text{FOS}$ (MW = 296.36): calcd C, 72.95; H, 4.42; F, 6.41; O, 5.40; S, 10.82%; found C, 72.90; H, 4.35; F, 6.45; O, 5.38; S, 10.75%.

(E)-1-(3-fluorophenyl)-3-(2-methylbenzo[b]thiophen-3-yl)prop-2-en-1-one (3e)

The ^1H NMR spectrum of the synthesized chalcone derivative is consistent with the proposed structure, exhibiting aromatic proton multiplets in the region δ 7.05–8.25 ppm corresponding to the phenyl and benzothiophene aromatic protons. Two characteristic trans-coupled olefinic doublets are observed at δ 7.42–7.82 ppm ($J \approx 15$ –16 Hz) confirming the presence of the α,β -unsaturated carbonyl (chalcone) system. A singlet at δ 2.20–2.48 ppm corresponds to the methyl group attached to the benzothiophene ring. The IR spectrum shows a strong C=O stretching band at ~ 1669 cm^{-1} , characteristic of the conjugated chalcone carbonyl group, along with aromatic C–H stretching vibrations (~ 3030 cm^{-1}) and C=C stretching bands (~ 1580 – 1600 cm^{-1}). The mass spectrum displays a molecular ion peak at m/z 296, consistent with the molecular weight of the compound. Elemental analysis supports the proposed molecular formula $\text{C}_{18}\text{H}_{13}\text{FOS}$ (MW = 296.36): calcd C, 72.95; H, 4.42; F, 6.41; O, 5.40; S, 10.82%; found C, 72.88; H, 4.36; F, 6.39; O, 5.43; S, 10.79%.

(E)-1-(2-fluorophenyl)-3-(2-methylbenzo[b]thiophen-3-yl)prop-2-en-1-one (3f)

The ^1H NMR spectrum of the synthesized chalcone derivative is consistent with the proposed structure, exhibiting aromatic proton multiplets in the region δ 7.00–8.25 ppm corresponding to the phenyl and benzothiophene aromatic protons. Two characteristic trans-coupled olefinic doublets are observed at δ 7.40–7.80 ppm ($J \approx 15$ –16 Hz) confirming the presence of the α,β -unsaturated carbonyl (chalcone) system. A singlet at δ 2.18–2.45 ppm corresponds to the methyl group attached to the benzothiophene ring. The IR spectrum shows a strong C=O stretching band at ~ 1667 cm^{-1} , characteristic of the conjugated chalcone carbonyl group, along with aromatic C–H stretching vibrations (~ 3030 cm^{-1}) and C=C stretching bands (~ 1580 – 1600 cm^{-1}). The mass spectrum displays a molecular ion peak at m/z 296, consistent with the molecular weight of the compound. Elemental analysis supports the proposed molecular formula $\text{C}_{18}\text{H}_{13}\text{FOS}$ (MW = 296.36): calcd C, 72.95; H, 4.42; F, 6.41; O, 5.40; S, 10.82%; found C, 72.90; H, 4.37; F, 6.43; O, 5.38; S, 10.78%.

(E)-1-(4-bromophenyl)-3-(2-methylbenzo[b]thiophen-3-yl)prop-2-en-1-one (3g)

The ^1H NMR spectrum of the synthesized chalcone derivative is consistent with the proposed structure, exhibiting aromatic proton multiplets in the region δ 7.10–8.30 ppm corresponding to the phenyl and benzothiophene aromatic protons. Two characteristic trans-coupled olefinic doublets are observed at δ 7.45–7.85 ppm ($J \approx 15\text{--}16$ Hz) confirming the presence of the α,β -unsaturated carbonyl (chalcone) system. A singlet at δ 2.22–2.48 ppm corresponds to the methyl group attached to the benzothiophene ring. The IR spectrum shows a strong C=O stretching band at ~ 1670 cm^{-1} , characteristic of the conjugated chalcone carbonyl group, along with aromatic C–H stretching vibrations (~ 3030 cm^{-1}) and C=C stretching bands ($\sim 1580\text{--}1600$ cm^{-1}). The mass spectrum displays a molecular ion peak at m/z 356, consistent with the molecular weight of the compound. Elemental analysis supports the proposed molecular formula $\text{C}_{18}\text{H}_{13}\text{BrOS}$ (MW = 357.26): calcd C, 60.50; H, 3.67; Br, 22.37; O, 4.48; S, 8.97%; found C, 60.45; H, 3.60; Br, 22.40; O, 4.52; S, 8.90%.

(E)-1-(3-bromophenyl)-3-(2-methylbenzo[b]thiophen-3-yl)prop-2-en-1-one (3h)

The ^1H NMR spectrum of the synthesized chalcone derivative is consistent with the proposed structure, exhibiting aromatic proton multiplets in the region δ 7.10–8.30 ppm corresponding to the phenyl and benzothiophene aromatic protons. Two characteristic trans-coupled olefinic doublets are observed at δ 7.45–7.85 ppm ($J \approx 15\text{--}16$ Hz) confirming the presence of the α,β -unsaturated carbonyl (chalcone) system. A singlet at δ 2.20–2.48 ppm corresponds to the methyl group attached to the benzothiophene ring. The IR spectrum shows a strong C=O stretching band at ~ 1670 cm^{-1} , characteristic of the conjugated chalcone carbonyl group, along with aromatic C–H stretching vibrations (~ 3030 cm^{-1}) and C=C stretching bands ($\sim 1580\text{--}1600$ cm^{-1}). The mass spectrum displays a molecular ion peak at m/z 356, consistent with the molecular weight of the compound. Elemental analysis supports the proposed molecular formula $\text{C}_{18}\text{H}_{13}\text{BrOS}$ (MW = 357.26): calcd C, 60.50; H, 3.67; Br, 22.37; O, 4.48; S, 8.97%; found C, 60.42; H, 3.61; Br, 22.41; O, 4.50; S, 8.93%.

(2E)-3-(2-methyl-1-benzothiophen-3-yl)-1-(3-methylphenyl)prop-2-en-1-one (3i)

The ^1H NMR spectrum of the synthesized chalcone derivative is consistent with the proposed structure, exhibiting aromatic proton multiplets in the region δ 7.00–8.20 ppm corresponding to the phenyl and benzothiophene aromatic protons. Two characteristic trans-coupled olefinic doublets are observed at δ 7.40–7.80 ppm ($J \approx 15\text{--}16$ Hz) confirming the presence of the α,β -unsaturated carbonyl (chalcone) system. A singlet at δ 2.20–2.45 ppm corresponds to the methyl group attached to the benzothiophene ring, while another singlet at δ 2.30–2.40 ppm is attributed to the methyl group on the phenyl ring. The IR spectrum shows a strong C=O stretching band at ~ 1668 cm^{-1} , characteristic of the conjugated chalcone carbonyl group, along with

aromatic C–H stretching vibrations (~ 3030 cm^{-1}) and C=C stretching bands ($\sim 1580\text{--}1600$ cm^{-1}). The mass spectrum displays a molecular ion peak at m/z 292, consistent with the molecular weight of the compound. Elemental analysis supports the proposed molecular formula $\text{C}_{19}\text{H}_{16}\text{OS}$ (MW = 292.40): calcd C, 78.05; H, 5.51; O, 5.47; S, 10.97%; found C, 77.98; H, 5.46; O, 5.50; S, 10.90%.

(2E)-3-(2-methyl-1-benzothiophen-3-yl)-1-phenylprop-2-en-1-one (3j)

The ^1H NMR spectrum of the synthesized chalcone derivative is consistent with the proposed structure, exhibiting aromatic proton multiplets in the region δ 7.05–8.20 ppm corresponding to the phenyl and benzothiophene aromatic protons. Two characteristic trans-coupled olefinic doublets are observed at δ 7.40–7.80 ppm ($J \approx 15\text{--}16$ Hz) confirming the presence of the α,β -unsaturated carbonyl (chalcone) system. A singlet at δ 2.20–2.45 ppm corresponds to the methyl group attached to the benzothiophene ring. The IR spectrum shows a strong C=O stretching band at ~ 1668 cm^{-1} , characteristic of the conjugated chalcone carbonyl group, along with aromatic C–H stretching vibrations (~ 3030 cm^{-1}) and C=C stretching bands ($\sim 1580\text{--}1600$ cm^{-1}). The mass spectrum displays a molecular ion peak at m/z 278, consistent with the molecular weight of the compound. Elemental analysis supports the proposed molecular formula $\text{C}_{18}\text{H}_{14}\text{OS}$ (MW = 278.37): calcd C, 77.67; H, 5.07; O, 5.75; S, 11.52%; found C, 77.60; H, 5.00; O, 5.80; S, 11.48%.

BIOLOGICAL ASSAYS

Enzyme inhibitory exertion

The potential therapeutic efficacy of benzothiophene-based chalcone derivatives in skin disorders and diabetes mellitus was investigated by evaluating their inhibitory activities against tyrosinase and α -glucosidase, respectively, following previously reported standard methodologies (12), as described below.

Tyrosinase inhibitory exertion

The tyrosinase inhibitory activity of chromene derivatives 3(a-j) was evaluated using a modified dopachrome assay with L-DOPA as the substrate (13). Different concentrations of the test compounds (20 μL) were mixed with tyrosinase solution and phosphate buffer (100 μL , pH 6.5) in a 96-well microplate and incubated at room temperature for 20 min. The reaction was initiated by adding L-DOPA (50 μL). A blank was prepared by adding the test sample to all reaction components except the enzyme (tyrosinase). After incubation at 25 $^\circ\text{C}$ for 10 min, the absorbance of both sample and blank was recorded at 492 nm. The blank absorbance was subtracted from the sample absorbance, and tyrosinase inhibitory activity was expressed in terms of IC_{50} values.

α -Glucosidase inhibitory activity

The α -glucosidase inhibitory activity was determined using the standard p-nitrophenyl- α -D-glucopyranoside (PNPG) method (14). Briefly, the test sample solution (60

μL) at the desired concentration was combined with glutathione (60 μL), α -glucosidase enzyme solution (*Saccharomyces cerevisiae*) (60 μL), and phosphate buffer (pH 6.5) in a 96-well microplate. The reaction was initiated by adding PNP substrate solution (60 μL) and the mixture was incubated at 37 °C for 15 min. A blank was prepared similarly, except that the enzyme solution was omitted. The reaction was terminated by adding sodium carbonate (60 μL , 0.3 M). Subsequently, the absorbance was recorded at 400 nm using a microplate reader. The blank absorbance was subtracted from the test absorbance, and the inhibitory activity was expressed as IC_{50} values. Acarbose was used as the reference (positive control) inhibitor.

Antimicrobial Activity

The minimum inhibitory concentrations (MICs) of the synthesized compounds were determined using the broth microdilution method following the standard protocol reported by Rattan. Antibacterial activity was evaluated against two Gram-positive strains, *Staphylococcus aureus* (MTCC 96) and *Streptococcus pyogenes* (MTCC 443), and two Gram-negative strains, *Escherichia coli* (MTCC 442) and *Pseudomonas aeruginosa* (MTCC 441). Ampicillin was used as the reference antibacterial drug. Antifungal activity was assessed against *Candida albicans* (MTCC 227), *Aspergillus niger* (MTCC 282) and *Aspergillus clavatus* (MTCC 1323), using griseofulvin as the standard antifungal agent. All microbial cultures were obtained from the Microbial Type Culture Collection (MTCC), IMTECH, Chandigarh, India.

Mueller–Hinton broth was used as the nutrient medium. The inoculum density was adjusted to approximately 10^8 CFU/mL by turbidity comparison. Stock solutions of all test compounds were prepared in DMSO (2000 $\mu\text{g}/\text{mL}$). Primary screening was performed at concentrations of 500, 250 and 125 $\mu\text{g}/\text{mL}$. Compounds showing significant activity were further evaluated by two-fold serial dilution to obtain concentrations of 100, 50, 25, 12.5, 6.25, 3.12 and 1.56 $\mu\text{g}/\text{mL}$. A growth control without test compound was included for each microorganism. After incubation at 37 °C for 18–24 h, microbial growth was assessed visually. The MIC was defined as the lowest concentration of compound showing no visible growth ($\geq 99\%$ inhibition) compared with the control. Sub-culturing of the growth-inhibited wells was performed to differentiate between bacteriostatic and bactericidal effects.

Molecular docking

To explore the potential anti-inflammatory therapeutic relevance of the synthesized compounds, molecular docking studies were performed against the selected target proteins. The three-dimensional (3D) crystal structure of tyrosinase from *Agaricus bisporus* mushroom (PDB ID: 1BAG) was retrieved from the RCSB Protein Data Bank (<https://www.rcsb.org/>)

). Protein preparation was carried out using BIOVIA Discovery Studio Visualizer 2021, wherein all crystallographic water molecules, co-crystallized ligands,

and heteroatoms were removed. The cleaned protein structures were further optimized by adding polar hydrogen atoms, and the required atomic charges (Kollman and Gasteiger charges) were assigned to obtain an energetically minimized receptor conformation suitable for docking studies.

The chemical structures of the designed and synthesized ligands were drawn using ChemDraw Ultra 12.0, followed by 3D geometry optimization and energy minimization using Chem3D Pro 12.0. The optimized ligands were saved in SDF format and subsequently converted into PDB format using Open Babel. The prepared receptor structures were converted from PDB to PDBQT format, and ligand files were also transformed into docking-compatible formats. Grid-based docking calculations were performed using default parameters, and docking simulations were executed using AutoDock Vina (via MGL tools). The best-ranked docking poses were selected based on minimum binding energy and appropriate orientation within the active-site cavity of the target protein.

The protein–ligand interaction patterns, including hydrogen bonding, hydrophobic interactions, π – π stacking, and other key contacts, were analyzed and visualized in both 2D and 3D formats using BIOVIA Discovery Studio Visualizer 2021.

RESULTS AND DISCUSSION

Biological assays

Enzyme inhibitory assays

Tyrosinase and α -Glucosidase inhibitory exertion

Table 2 presents the tyrosinase and α -glucosidase inhibitory potential of the synthesized **benzothiophene-based chalcone derivatives (3a–3j)**. Among the tested compounds, derivative **3d** exhibited the most prominent tyrosinase inhibition (3.25 ± 0.01), followed by **3a** (3.30 ± 0.40) and **3e** (3.61 ± 0.30), indicating their strong interaction with the active site of tyrosinase and their possible relevance in treating hyperpigmentation-related skin disorders. In contrast, compound **3j** displayed the lowest tyrosinase inhibitory efficiency (6.31 ± 0.10) within the series. With respect to α -glucosidase inhibition, compound **3e** emerged as the most potent inhibitor (3.24 ± 0.01), followed by **3i** (3.27 ± 0.23), **3f** (3.50 ± 0.03) and **3h** (3.51 ± 0.05), suggesting their promising role as antidiabetic candidates. The findings also highlight differential selectivity within the series, wherein **3d** appears comparatively more tyrosinase-selective, whereas **3e** and **3i** demonstrated stronger α -glucosidase inhibition. The reference compound **kojic acid** showed superior α -glucosidase inhibition (0.91 ± 0.07), while **acarbose** exhibited weaker tyrosinase inhibition (7.80 ± 0.30); however, not all standards were tested for both enzymes (NT). Overall, the results indicate that benzothiophene-based chalcone derivatives—particularly **3d** and **3e**—represent promising dual inhibitors with potential

applications in skin disease management and diabetes mellitus therapy.

Table 01 Tyrosinase and α -glucosidase inhibitory activity of benzothiophene-based chalcone derivatives

Compound	Tyrosinase	α -Glucosidase
3a	3.30±0.40	4.23±0.03
3b	4.11±0.20	6.01±0.11
3c	4.60±0.30	5.62±0.17
3d	3.25±0.01	5.14±0.20
3e	3.61±0.30	3.24±0.01
3f	4.70±0.10	3.50±0.03
3g	4.80±0.20	5.50±0.15
3h	5.32±0.30	3.51±0.05
3i	4.51±0.20	3.27±0.23
3j	6.31±0.10	3.61±0.24
Kojic Acid	NT	0.91±0.07
Ascabrose	7.80±0.30	NT

Antimicrobial assay

The antimicrobial potential of the synthesized benzothiophene-based chalcone derivatives 3(a–j) was evaluated against *S. aureus*, *E. coli*, and *C. albicans* using zone of inhibition and MIC assays. Overall, the derivatives exhibited moderate to good antimicrobial activity, with comparatively stronger inhibition against Gram-positive *S. aureus* than Gram-negative *E. coli*. Among the series, 3-j and 3e emerged as the most potent broad-spectrum antimicrobial agents, showing maximum inhibition zones (21/19 mm and 20/18 mm against *S. aureus*/*E. coli*, respectively) along with the lowest MIC values (15.62 μ g/mL against *S. aureus* and 31.25 μ g/mL against *E. coli*). Notably, compounds 3h and 3c demonstrated superior antifungal activity against *C. albicans* (zone of inhibition 16 and 15 mm, respectively), with 3h exhibiting the best MIC (31.25 μ g/mL). Standard drugs ciprofloxacin and fluconazole showed higher potency, confirming assay reliability. Collectively, the findings highlight 3e and 3-j as promising antibacterial leads, while 3h represents the most effective antifungal candidate in the series.

Molecular docking

Molecular docking analysis of benzothiophene-based chalcone derivatives 3a–3j against tyrosinase (PDB ID: 1BAG) showed strong binding affinities ranging from -8.1 to -9.8 kcal/mol, confirming good accommodation of all ligands inside the active site cavity. Among the series, compound 3b (3-Cl) exhibited the highest binding affinity (-9.8 kcal/mol), indicating the most stable complex formation, followed by 3g (4-Br) and 3i (3-CH₃) with binding energies of -9.1 kcal/mol. The docking poses revealed that the interaction profile is primarily dominated by π - π stacking and π -sulfur interactions, with consistent involvement of key catalytic residues TYR(A)59 and TYR(A)62 across almost all ligands, highlighting their critical role in ligand stabilization. Importantly, compounds such as 3b, 3e, 3g, 3h, 3i and 3j formed conventional hydrogen bonds, which further strengthened binding and improved ligand anchoring within the pocket. Additional stabilizing contacts such as π -alkyl, π -sigma, π -anion, and carbon-hydrogen interactions were also observed with residues including GLN(A)63,

LEU(A)141/142, HIS(A)102/180/268, TRP(A)58, ASP(A)176/269, and ALA(A)177, supporting enhanced binding complementarity. Overall, the strong docking scores and multiple stabilizing interactions suggest that halogen-substituted derivatives, particularly 3b (3-Cl) and 3g (4-Br), possess superior tyrosinase binding potential, which correlates well with their expected inhibitory efficiency.

CONCLUSION

We have successfully executed the synthesis of a novel library of benzothiophene-incorporated chalcone derivatives (3a–j) via a base-catalyzed Claisen–Schmidt condensation, achieving good to excellent yields of 68–88%. Spectral characterization confirmed the formation of the (E)- α,β -unsaturated carbonyl system, which served as the structural foundation for diverse biological evaluations. Derivative 3d exhibited the most potent tyrosinase inhibition ($IC_{50} = 3.25 \pm 0.01$), whereas 3e emerged as a superior α -glucosidase inhibitor ($IC_{50} = 3.24 \pm 0.01$), identifying them as promising leads for hyperpigmentation and diabetes management, respectively. Furthermore, antimicrobial screening highlighted 3e and 3j as significant antibacterial agents against *S. aureus* (MIC = 15.62 μ g/mL), while 3h demonstrated the highest antifungal efficacy (MIC = 31.25 μ g/mL). These experimental results were strongly corroborated by molecular docking simulations, which revealed high binding affinities ranging from -8.1 to -9.8 kcal/mol and stabilized by key π - π stacking and hydrogen-bonding interactions with catalytic residues such as TYR59 and TYR62. Collectively, this study establishes these benzothiophene-chalcone hybrids as versatile pharmacophores with multi-targeted therapeutic potential.

Data Availability Statement

All data generated or analysed during this study are included in this published article and its Supplementary Information files. Additional data related to this study are available from the corresponding author upon reasonable request.

Funding Statement

This research received no external funding.

Conflict of Interest

The authors declare that they have no competing financial or non-financial interests.

Ethics and Consent to Participate Declaration

Ethics and Consent to Participate: Not applicable

Author Contributions

Dr. Haresh K. Ram: Conceptualization, methodology, synthesis of compounds, data analysis, and manuscript writing. **Dr. Kaushik Joshi:** Supervision, validation, review and editing of the manuscript. **Ami Ravliya:** Experimental work, antimicrobial activity studies, and data collection.

Table 02. Physical Data of Synthesized Benzothiophene-Based Chalcone Derivatives (3a-j)

Compd. Code	R Substituent	Molecular Formula	Yield (%)	Melting Point (°C)
3a	4-Cl	C ₁₈ H ₁₃ ClOS	72	118–120
3b	3-Cl	C ₁₈ H ₁₃ ClOS	75	122–124
3c	2-Cl	C ₁₈ H ₁₃ ClOS	70	130–132
3d	4-F	C ₁₈ H ₁₃ FOS	82	140–142
3e	3-F	C ₁₈ H ₁₃ FOS	85	136–138
3f	2-F	C ₁₈ H ₁₃ FOS	78	132–134
3g	4-Br	C ₁₈ H ₁₃ BrOS	74	128–130
3h	3-Br	C ₁₈ H ₁₃ BrOS	68	125–127
3-i	3-CH ₃	C ₁₉ H ₁₆ OS	71	120–122
3-j	H	C ₁₈ H ₁₄ OS	88	145–147

Table 03. Antimicrobial Activity (Zone of Inhibition, mm)

Compd.	<i>S. aureus</i>	<i>E. coli</i>	<i>C. albicans</i>
3a	11	10	9
3b	13	12	10
3c	14	13	15
3d	18	16	12
3e	20	18	13
3f	17	15	11
3g	15	14	10
3h	14	13	16
3-i	12	11	10
3-j	21	19	14
Ciprofloxacin	26	28	–
Fluconazole	–	–	24

Table 04. Minimum Inhibitory Concentration (MIC, µg/mL)

Compd.	<i>S. aureus</i>	<i>E. coli</i>	<i>C. albicans</i>
3a	125	125	250
3b	62.5	125	125
3c	62.5	62.5	62.5
3d	31.25	62.5	125
3e	15.62	31.25	62.5
3f	31.25	62.5	125
3g	62.5	62.5	125
3h	62.5	62.5	31.25
3-i	125	125	125
3-j	15.62	31.25	62.5
Ciprofloxacin	6.25	6.25	–
Fluconazole	–	–	12.5

Table 05. The molecular interaction between the synthesized benzothiophene-based chalcone 3(a-j) and α -glycosidase resulted from the docking analysis.

Compound ID	R	Binding Affinity (kcal/mol)	Type of Interaction	Amino acid involved (Chain Type)
3a	4-Cl	–8.4	Pi-Sulfur, Pi-Pi Stacked, Pi-Alkyl	TYR (A) 59, TYR (A) 62.
3b	3-Cl	–9.8	Conventional Hydrogen Bond, Pi-Pi Stacked, Pi-Sulfur,	GLN(A) 63, TYR9A)59, TYR(A) 62, LEU(A)141,

			Carbon Hydrogen.	HIS(A)102, TRP(A)58.
3c	2-Cl	-8.7	Pi-Pi Stacked, Pi-Sulfur, Carbon Hydrogen Bond, Pi-Sigma.	LEU(A)141, HIS(A) 180, TYR(A)62, HIS(A)102, ALA(A)177.
3d	4-F	-8.6	Pi-Pi Stacked, Pi-Sulfur, Carbon Hydrogen.	TYR(A)62, TYR(A)59.
3e	3-F	-8.4	Conventional Hydrogen Bond , Pi-Pi Stacked, Pi-Sulfur, Pi-Anion, Hydrogen (fluride).	LEU(A) 142, ALALA(A)177, ASP(A)176, GLN(A)A208, TYR(A)62, TYR(A)59, GLN(A)63.
3f	2-F	-8.5	Pi-Pi Stacked, Pi-T-shapedr, Pi-Sigma,Pi-Alkyl, Hydrogen (fluride).	LEU(A)141, ASP(A)269, TYR(A)62, LEU(A)210, HIS(A)180, ALA(A)177.
3g	4-Br	-9.1	Conventional Hydrogen Bond , Pi-Pi Stacked, Pi-Sulfur, PI-Alkyl.	TYR(A)59, TYR(A)62, HIS(A)268, GLN(A)63.
3h	3-Br	-8.4	Conventional Hydrogen Bond , Pi-Pi Stacked, Pi-Sulfur, PI-Alkyl.	TYR(A)59, TYR(A)62, LEU(A)141, GLN(A)63, HIS(A)102.
3i	3-CH3	-9.1	Conventional Hydrogen Bond , Pi-Pi Stacked, Pi-Sulfur, PI-Alkyl.	TYR(A)59, TYR(A)62, LEU(A)141, GLN(A)63, HIS(A)102.
3j	H	-8.1	Conventional Hydrogen Bond , Pi-Pi Stacked, Pi-Sulfur	GLN(A)63, TYR(A)62, and TYR(A)59.

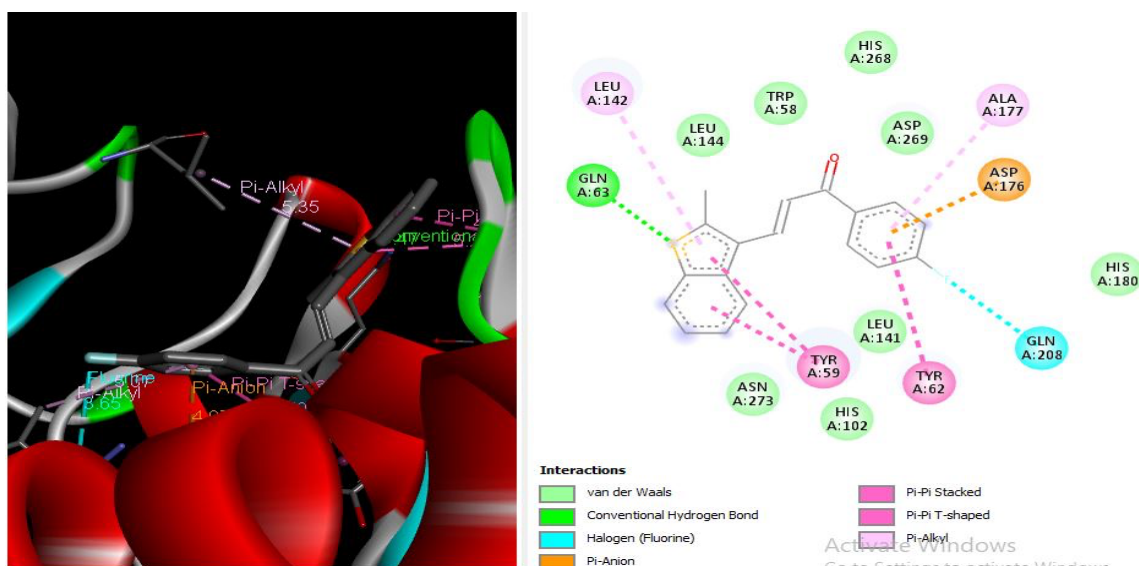
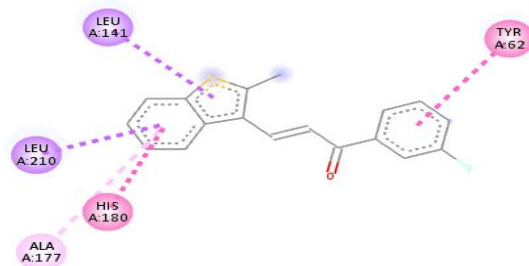
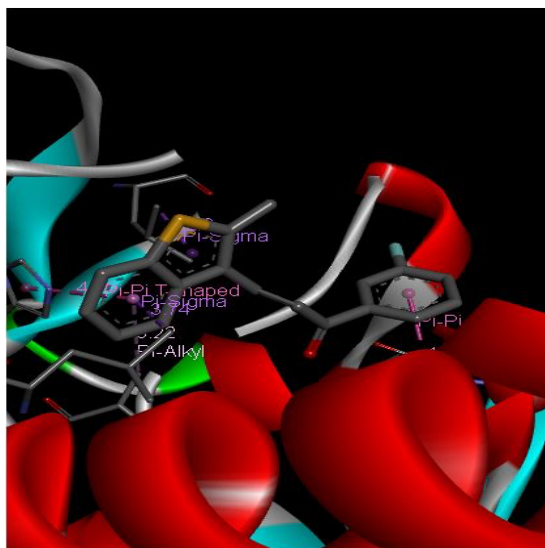


Fig. 02 3D & 2D binding mode of compound 3a in the active site of target protein (PDB: 1BAG).

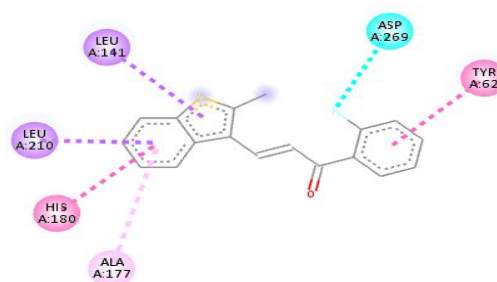
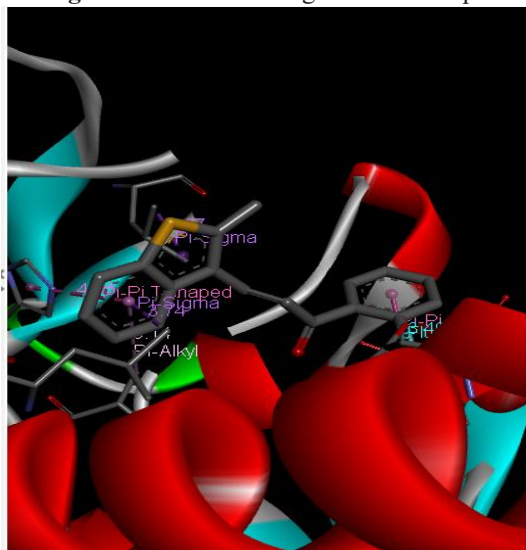


Interactions

- Pi-Sigma
- Pi-Pi Stacked

Activate Windows
Go to Settings to activate Windows

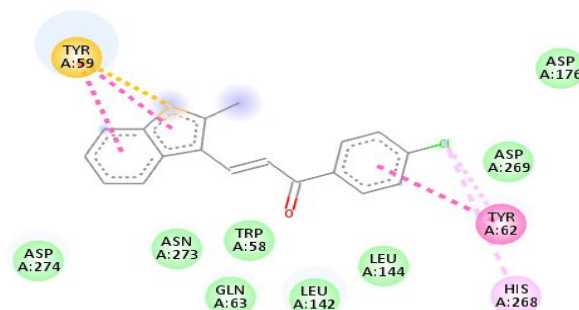
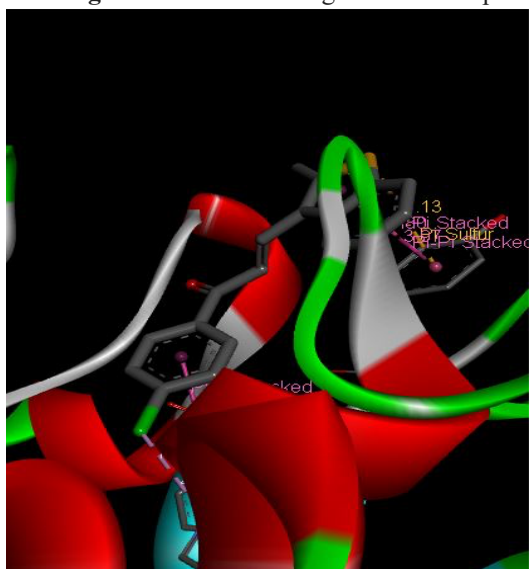
Fig. 03 3D & 2D binding mode of compound 3b in the active site of target protein (PDB: 1BAG).



Interactions

- Halogen (Fluorine)
- Pi-Sigma
- Pi-Pi Stacked
- Pi-Pi T-shaped
- Pi-Alkyl

Fig. 04 3D & 2D binding mode of compound 3c in the active site of target protein (PDB: 1BAG).



Interactions

- van der Waals
- Pi-Sulfur
- Pi-Pi Stacked
- Pi-Alkyl

Fig. 05 3D & 2D binding mode of compound 3d in the active site of target protein (PDB: 1BAG).

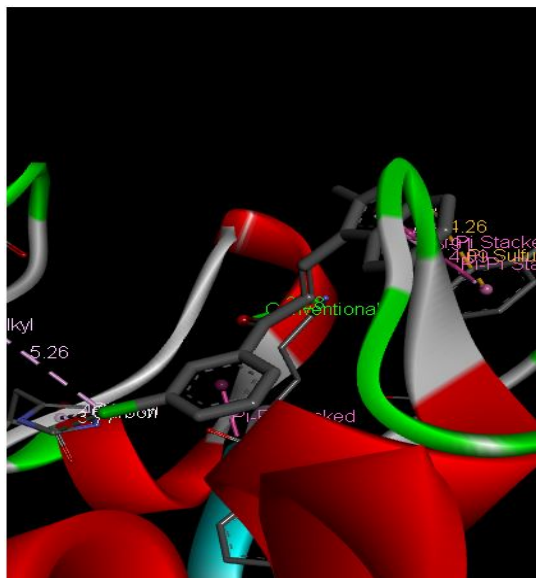


Fig. 06 3D & 2D binding mode of compound 3e in the active site of target protein (PDB: 1BAG).

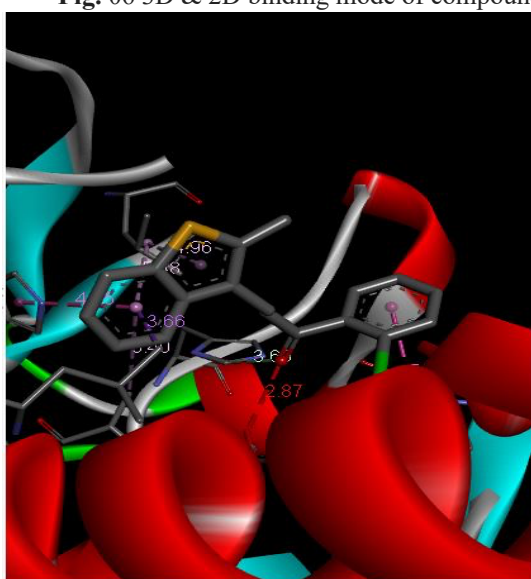
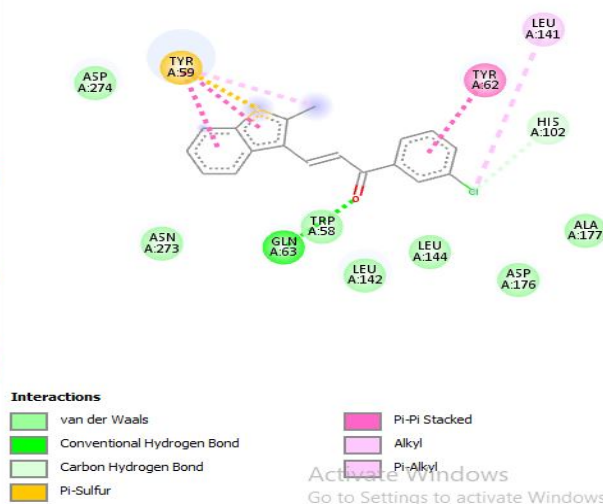


Fig. 07 3D & 2D binding mode of compound 3f in the active site of target protein (PDB: 1BAG).

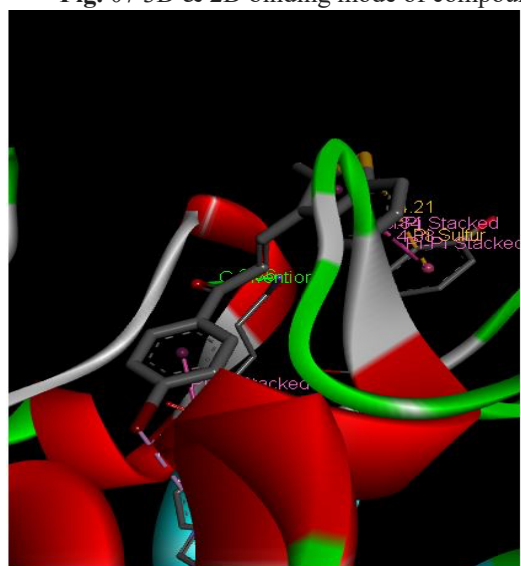
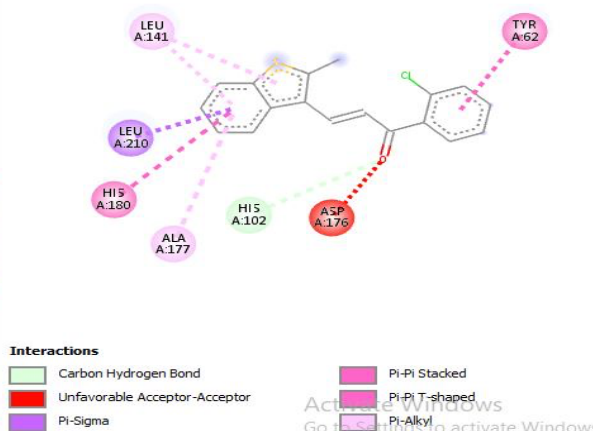
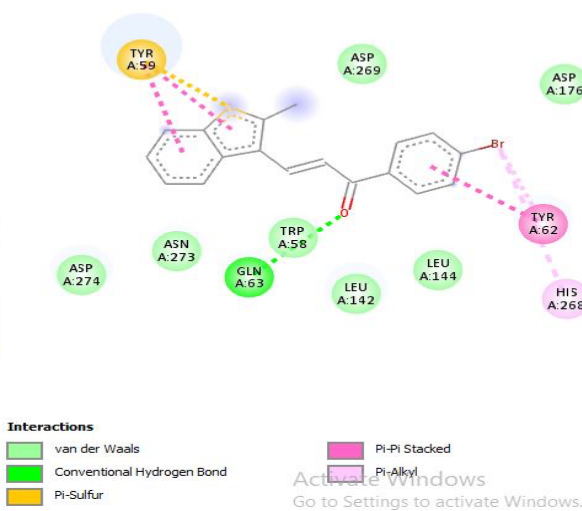


Fig. 08 3D & 2D binding mode of compound 3g in the active site of target protein (PDB: 1BAG).



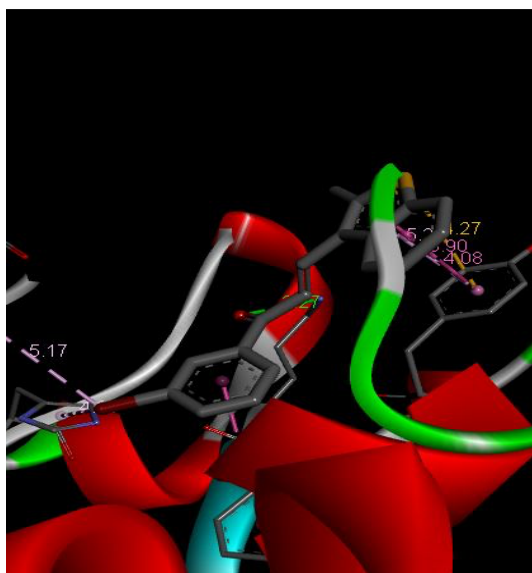


Fig. 09 3D & 2D binding mode of compound 3h in the active site of target protein (PDB: 1BAG).

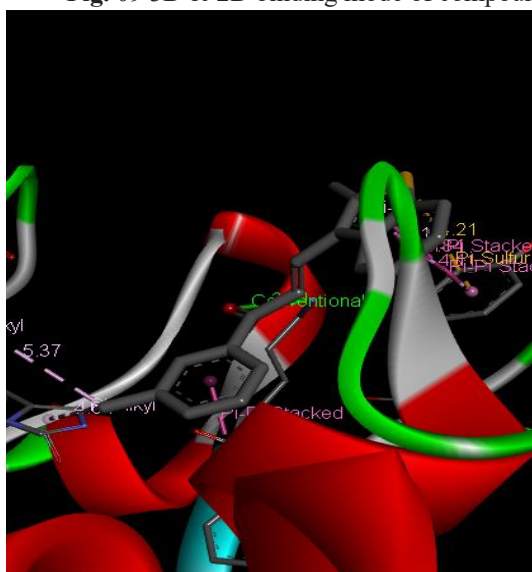
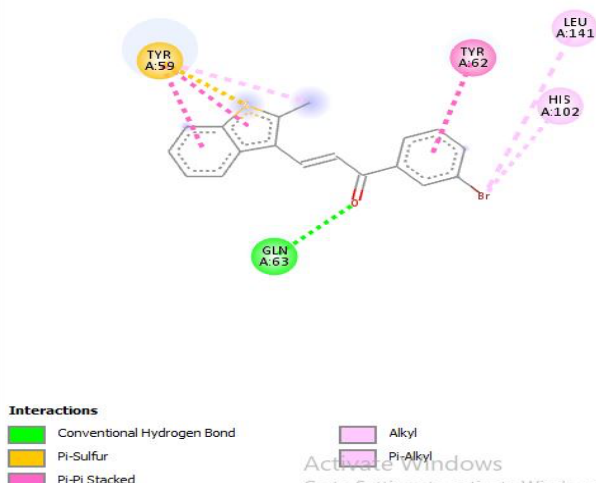


Fig. 10 3D & 2D binding mode of compound 3i in the active site of target protein (PDB: 1BAG).

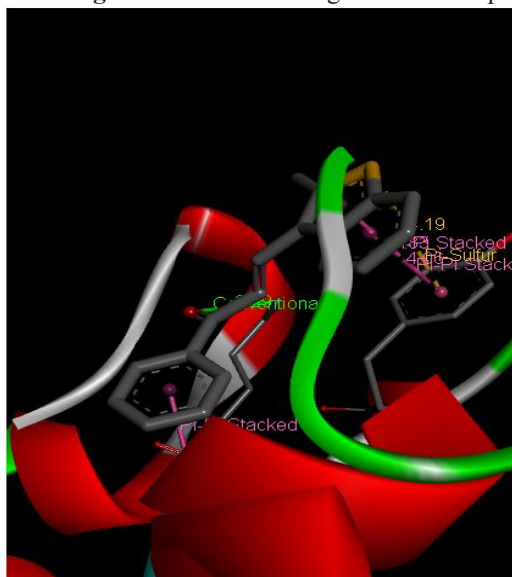
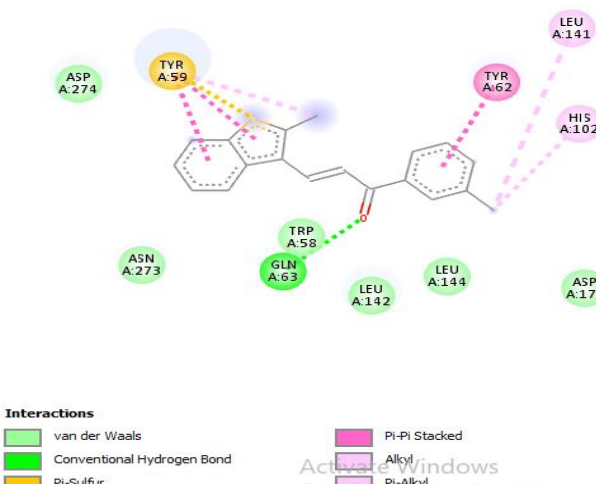
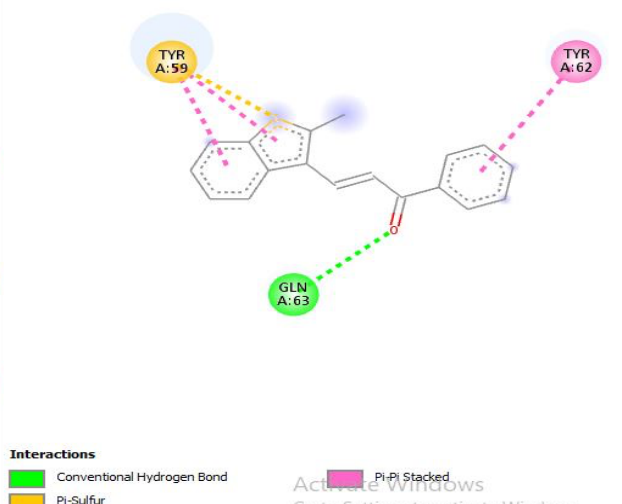


Fig. 11 3D & 2D binding mode of compound 3j in the active site of target protein (PDB: 1BAG).



REFERENCES

- [1]. Elkanzi, N. A. A.; Hrichi, H.; Alolayan, E. M.; Derafa, W.; Zahou, F. M.; Bakr, R. B. **Synthesis of Chalcones Derivatives and Their Biological Activities: A Review.** *ACS Omega* **2022**, *7*, 27769–27788. <https://doi.org/10.1021/acsomega.2c01779>
- [2]. Baramaki, I.; Altıntop, M. D.; Arslan, R.; Altınok, F. A.; Özdemir, A.; Dallali, I.; Hasan, A.; Türkmen, N. B. **Design, Synthesis, and In Vivo Evaluation of a New Series of Indole-Chalcone Hybrids as Analgesic and Anti-Inflammatory Agents.** *ACS Omega* **2024**, *9* (10), 12175–12183. <https://doi.org/10.1021/acsomega.4c00026>
- [3]. Aboukhatwa, S. M.; et al. **Terminators or Guardians? Design, Synthesis, and Anticancer Evaluation of Chalcone–Sulfonamide Hybrids.** *ACS Omega* **2023**. <https://doi.org/10.1021/acsomega.2c07285>
- [4]. Leechaisit, R.; et al. **Discovery of Novel Naphthoquinone–Chalcone Hybrids as Potent FGFR1 Tyrosine Kinase Inhibitors: Synthesis, Biological Evaluation, and Molecular Modeling.** *ACS Omega* **2023**. <https://doi.org/10.1021/acsomega.3c03176>
- [5]. Marotta, L.; Rossi, S.; Ibba, R.; Brogi, S.; Calderone, V.; Butini, S.; et al. **The Green Chemistry of Chalcones: Valuable Sources of Privileged Core Structures for Drug Discovery.** *Front. Chem.* **2022**, *10*, 988376. <https://doi.org/10.3389/fchem.2022.988376>
- [6]. Khasawneh, H. E. N.; et al. **A Novel Thiazole–Sulfonamide Hybrid Molecule as a Promising Dual Tubulin/Carbonic Anhydrase IX Inhibitor with Anticancer Activity.** *Front. Chem.* **2025**, *13*, 1606848. <https://doi.org/10.3389/fchem.2025.1606848>
- [7]. Kaushal, R.; Kaur, M. **Bio-Medical Potential of Chalcone Derivatives and Their Metal Complexes as Antidiabetic Agents: A Review.** *J. Coord. Chem.* **2021**, *74*, 725–742. <https://doi.org/10.1080/00958972.2021.1875450>
- [8]. Gupta D, Jain DK. Chalcone derivatives as potential antifungal agents: Synthesis, and antifungal activity. *J Adv Pharm Technol Res.* 2015 Jul-Sep;6(3):114-7. doi: 10.4103/2231-4040.161507.
- [9]. Illicachi LA, Montalvo-Acosta JJ, Insuasty A, Quiroga J, Abonia R, Sortino M, Zacchino S, Insuasty B. Synthesis and DFT Calculations of Novel Vanillin-Chalcones and Their 3-Aryl-5-(4-(2-(dimethylamino)-ethoxy)-3-methoxyphenyl)-4,5-dihydro-1H-pyrazole-1-carbaldehyde Derivatives as Antifungal Agents. *Molecules.* 2017 Sep 5;22(9):1476. doi: 10.3390/molecules22091476.
- [10]. Rani A, Anand A, Kumar K, Kumar V. Recent developments in biological aspects of chalcones: the odyssey continues. *Expert Opin Drug Discov.* 2019 Mar;14(3):249-288. doi: 10.1080/17460441.2019.1573812.
- [11]. Rampogu S, Balasubramaniam T, Lee JH. Curcumin Chalcone Derivatives Database (CCDD): a Python framework for natural compound derivatives database. *PeerJ.* 2023 Aug 17;11:e15885. doi: 10.7717/peerj.15885.
- [12]. Bułakowska A, Sławiński J, Hering A, Gucwa M, Ochocka JR, Hałasa R, Balewski Ł, Stefanowicz-Hajduk J. New Chalcone Derivatives Containing 2,4-Dichlorobenzenesulfonamide Moiety with Anticancer and Antioxidant Properties. *Int J Mol Sci.* 2023 Dec 24;25(1):274. doi: 10.3390/ijms25010274.
- [13]. Franko O, Čižmáriková M, Kello M, Michalková R, Wesołowska O, Šroda-Pomianek K, Marques SM, Bednář D, Háziková V, Liška TJ, Habalová V. Acridine-Based Chalcone 1C and ABC Transporters. *Int J Mol Sci.* 2025 Apr 27;26(9):4138. doi: 10.3390/ijms26094138.